Dyes and Pigments 163 (2019) 371–380

Contents lists available at ScienceDirect

Dyes and Pigments

journal homepage: www.elsevier.com/locate/dyepig

Efficient synthesis of high solid content emulsions of AIE polymeric nanoparticles with tunable brightness and surface functionalization through miniemulsion polymerization

Xiaoqin Liang[a], Yaxin Hu[a], Zhihai Cao[a,*], Lisheng Xiao[a], Junjie Lou[a], Ling Liu[a], Yijia Wang[a], Zujin Zhao[b,**], Dongming Qi[a], Qinmin Cui[c,***]

[a] Key Laboratory of Advanced Textile Materials and Manufacturing Technology and Engineering Research Center for Eco-Dyeing & Finishing of Textiles, Ministry of Education, Zhejiang Sci-Tech University, Hangzhou, 310018, China
[b] State Key Laboratory of Luminescent Materials and Devices, South China University of Technology, Guangzhou, 510640, China
[c] School of Pharmacy, Hangzhou Medical College, 481 Binwen Road, Hangzhou, 310053, China

ARTICLE INFO

Keywords:
Aggregation-induced emission
Miniemulsion polymerization
AIE polymeric nanoparticles
High solid content
Surface functionalization

ABSTRACT

Efficient production and flexible surface functionalization are important developing directions for the synthesis of polymeric nanomaterials. In this work, aggregation-induced emission (AIE) polymeric nanoparticles (PNPs) were efficiently synthesized by encapsulating a model AIE luminogen, tetraphenylethylene (TPE), within a polymeric matrix via miniemulsion polymerization. The AIE PNPs with similar emission and particle properties were synthesized in a wide solid content range of 8–40 wt%. The particle size and photoluminescence intensity of AIE PNPs could be flexibly tuned by synthetic parameters including the surfactant content and TPE content. Furthermore, the surface carboxyl- and amino-functionalization of AIE PNPs were conveniently achieved through copolymerization of styrene and functional monomers methacrylic acid and 2-aminoethyl methacrylate hydrochloride, respectively, in miniemulsions. The surface functionalization extent could be facilely tuned by the content of functional monomers. This miniemulsion polymerization based technique could be a feasible and efficient method to prepare AIE PNPs with versatile surface functionalization, tunable brightness, and controllable particle properties for the applications in biodetection, bioimaging, etc.

1. Introduction

In recent years, fluorescent nanomaterials have gained great attention due to their wide applications in fields of biology, therapeutics, optoelectronic devices, and diagnostics [1–9]. Incorporation of luminogens into polymeric nanoparticles (PNPs) is of great interest because fluorescent PNPs show more advantages in terms of brightness, photostability, and functionalization compare to pristine luminogens [10]. Among various organic luminogens, those with aggregation-induced emission (AIE) properties have acquired particular popularity because of their enhanced emission in the solid state or crystals, which can elegantly conquer the aggregation-caused quenching (ACQ) effect of traditional organic chromophores [11–13].

So far, a variety of AIE PNPs have drawn extensive interests on account of their remarkable stability in biological environments and well-controlled surface properties [10,14,15]. These AIE PNPs can be prepared through a number of innovative strategies including desolvation method [16], self-assembly of copolymers containing AIE moieties [17,18], host–guest supramolecular assembly [19], co-nanoprecipitation [20], semi-continuous polymerization [21], and emulsion polymerization [22,23]. For example, Wei's group developed a series of self-assembly based techniques that combined with RAFT polymerization, Schiff base condensation, Mannich reaction, multicomponent reaction, click polymerization, and dynamic bonding interaction, to prepare versatile AIE PNPs [24–29]. Nicolas et al. prepared AIE prodrug PNPs by co-nanoprecipitation of AIE polymers from nitroxide-mediated polymerization and polymeric prodrug [20]. However, most of these self-assembly based techniques include high cost synthesis of well-defined amphiphilic AIE-moiety-containing block copolymers or complicated post-functionalization through various organic reactions.

* Corresponding author.
** Corresponding author.
*** Corresponding author.
E-mail addresses: zhcao@zstu.edu.cn (Z. Cao), mszjzhao@scut.edu.cn (Z. Zhao), cuiqm@hmc.edu.cn (Q. Cui).

https://doi.org/10.1016/j.dyepig.2018.12.018
Received 1 November 2018; Received in revised form 6 December 2018; Accepted 11 December 2018
Available online 12 December 2018
0143-7208/

Furthermore, most of the reported techniques only allow to prepare AIE PNPs under a relatively low solid content. For example, Qin et al. prepared AIE luminogens (AIEgens)-loaded bovine serum albumin (BSA) PNPs through the desolvation method under a very low solid content [16]. Liu et al. carried out the emulsion polymerization at a solid content below 5 wt% to prepare AIE PNPs [22]. It is of great importance to synthesize AIE PNPs at a high level of solid content for efficient production [30].

However, preparation of high solid content emulsions may encounter many difficulties, like colloidal instability, uncontrolled particle size and particle size distribution, and increased viscosity. It has been reported that the miniemulsion polymerization technique could be readily used to prepare high solid content emulsions of various PNPs [31–38]. In a typical miniemulsion polymerization system, many monomer droplets with a size of several ten to several hundred nanometer are homogenously dispersed in an aqueous continuous phase. PNPs are mainly formed through droplet nucleation in the polymerization process. This technique can be used to prepare various functional PNPs through copolymerization of functional monomers or physical encapsulation of functional materials [39,40]. Recently, we reported that AIE PNPs could be successfully prepared through copolymerization of common monomers, like styrene (St) and methyl methacrylate, with an AIE functional monomer in water-borne miniemulsion systems [41,42]. The synthesized AIE PNPs displayed high brightness, good biocompatibility, and good cell staining ability. However, in our previous work, those AIE PNPs were synthesized at a relatively low solid content (8 wt% relative to water) [42]. Therefore, it is highly meaningful to tentatively synthesize AIE PNPs at a much higher solid content in miniemulsions.

Besides the efficient synthesis, it is equivalently important to undergo surface functionalization of AIE PNPs especially used for biological applications, which may endow AIE PNPs with improved biocompatibility, targeting ability, and enhanced *in vivo* circulation [10]. Prior to sophisticated functionalization, it is necessary to introduce some reactive functional groups like hydroxyl, carboxyl, or amino groups to the surface of AIE PNPs. These reactive groups may further experience coupling reactions with other functional components like targeting peptides, folic acid, and so on. Wei et al. reported that the surface of AIE PNPs could be functionalized with carboxyl groups through emulsion polymerization of styrene and acrylic acid [22]. However, in their report, they only discussed the contribution of surface carboxylated functionalization to the good water dispersibility of AIE PNPs. In miniemulsion polymerization systems, the preliminary surface functionalization of PNPs with hydroxyl, carboxyl, and amino groups could be realized through copolymerization of common monomers with functional vinyl monomers carrying various reactive groups [43,44]. The relationships between the functional monomer content and the surface carboxyl group density, particle size and its distribution, and surface charge state can guide us to better control the surface functionalization state of AIE PNPs, and provide a basis for further complex modification. However, to the best of our knowledge, as a novel application of miniemulsion polymerization in preparation of AIE PNPs, the surface functionalization of AIE PNPs with carboxyl or amino groups has not been thoroughly investigated yet.

In this work, AIE PNPs with and without surface functionalization were conveniently prepared through encapsulation of a model AIEgen, tetraphenylethylene (TPE), in water-borne miniemulsions (Scheme 1). The AIE PNPs displayed a well-defined spherical morphology and narrow particle size distribution. The brightness of AIE PNPs could be accurately regulated by changing the TPE content. The AIE PNPs with similar particle properties and emission ability could be synthesized in a wide solid content range of 8 − 40 wt%. Furthermore, surface carboxyl- or amino-functionalized AIE PNPs were synthesized through miniemulsion copolymerization of St with methacrylic acid (MAA) and 2-aminoethyl methacrylate hydrochloride (AEMH), respectively. According to the quantitative evaluation on the relationship between density of carboxyl or amino groups on the AIE PNP surface and the MAA or AEMH content, it was found that the surface functionalization extent could be readily tuned by the MAA or AEMH content.

2. Experimental section

2.1. Materials

TPE (95%) was obtained from Shanghai Aladdin Chemistry Co. Ltd. St (AR, Tianjin Yongda Chemical Reagent Co., Ltd.) was purified through reduced distillation, and stored in a refrigerator before use. MAA (CP, Shanghai Zhanyun Chemical Co., Ltd.) and AEMH (90%, J&K Scientific Co., Ltd.) were used as received. The non-ionic surfactant O-50, a poly(ethylene oxide)-hexadecyl ether with an ethylene oxide block length of ~50 units, was obtained from Jiangsu Hai'an Petrochemical Factory. *n*-Hexadecane (HD, 99%, Acros Organics), sodium dodecyl sulfate (SDS, CP, Shanghai Aladdin Chemistry Co., Ltd.), potassium persulfate (KPS, AR, Shanghai Aladdin Chemistry Co. Ltd.), 2,2'-azodiisobutyronitrile (AIBN, AR, Shanghai Aladdin Chemistry Co., Ltd.), H_2SO_4 (AR, Zhejiang Sanying Chemical Reagent Co., Ltd.), NaOH (AR, Tianjin Yongda Chemical Reagent Co., Ltd.), KBr (99.5%, Shanghai Aladdin Chemistry Co. Ltd.), and ethanol (AR, Hangzhou Gaojing Fine Chemical Co., Ltd.) were used as received. Self-made deionized water was and used in all experiments.

2.2. Preparation of PSt/TPE PNPs through miniemulsion polymerization

SDS was dissolved in water to form an aqueous solution. TPE was dissolved in a mixed solution of St and HD to form a hydrophobic solution. Both solutions were mixed and stirred with a rate of 700 rpm at 40 °C for 15 min to obtain a crude emulsion. Subsequently, the crude emulsion was sonicated at 400 W for 9 min by using a pulse mode (work 12 s, break 6 s) to form a monomer miniemulsion. After addition of KPS (0.05 g), the polymerization ran at 70 °C for 5 h with a continuous stirring of 400 rpm. The recipes for the prepared emulsions of PSt/TPE PNPs are listed in Table 1.

2.3. Preparation of surface functionalized PSt/TPE PNPs through miniemulsion polymerization

For preparation of surface carboxyl-functionalized PSt/TPE PNPs, the overall amount of St and MAA was kept at 10 g, and the MAA content was varied in the range of 0–10 wt%. MAA was directly mixed with St. The protocols of pre-emulsification, sonication, and polymerization were the same as those for the preparation of PSt/TPE PNPs. The emulsions of carboxyl-functionalized PSt/TPE PNPs were dialyzed in deionized water until the conductivity of the diffusate reached ~2 μS cm^{-1} to remove the surfactant. The recipes for the prepared emulsions of carboxyl-functionalized PSt/TPE PNPs are listed in Table 2.

Considering the potential cytotoxicity of cationic surfactants [45], the nonionic emulsifier O-50 was used to prepare surface amino-functionalized PSt/TPE PNPs through miniemulsion polymerization. The overall amount of St and AEMH was fixed at 1.0 g, and the AEMH content was varied in the range of 0–10 wt%. Due to the limited solubility of AEMH in hydrophobic monomers, both AEMH and O-50 were pre-dissolved in water. TPE and AIBN were dissolved in a mixed solution of St and HD to form a hydrophobic solution. The protocols of pre-emulsification and sonication were the same as those of the preparation of PSt/TPE PNPs. The polymerization ran for 20 h at 70 °C. The emulsions of amino-functionalized PSt/TPE PNPs were dialyzed in deionized water for 3 days to remove the surfactant. The recipes for the prepared emulsions of amino-functionalized PSt/TPE PNPs are listed in Table 3.

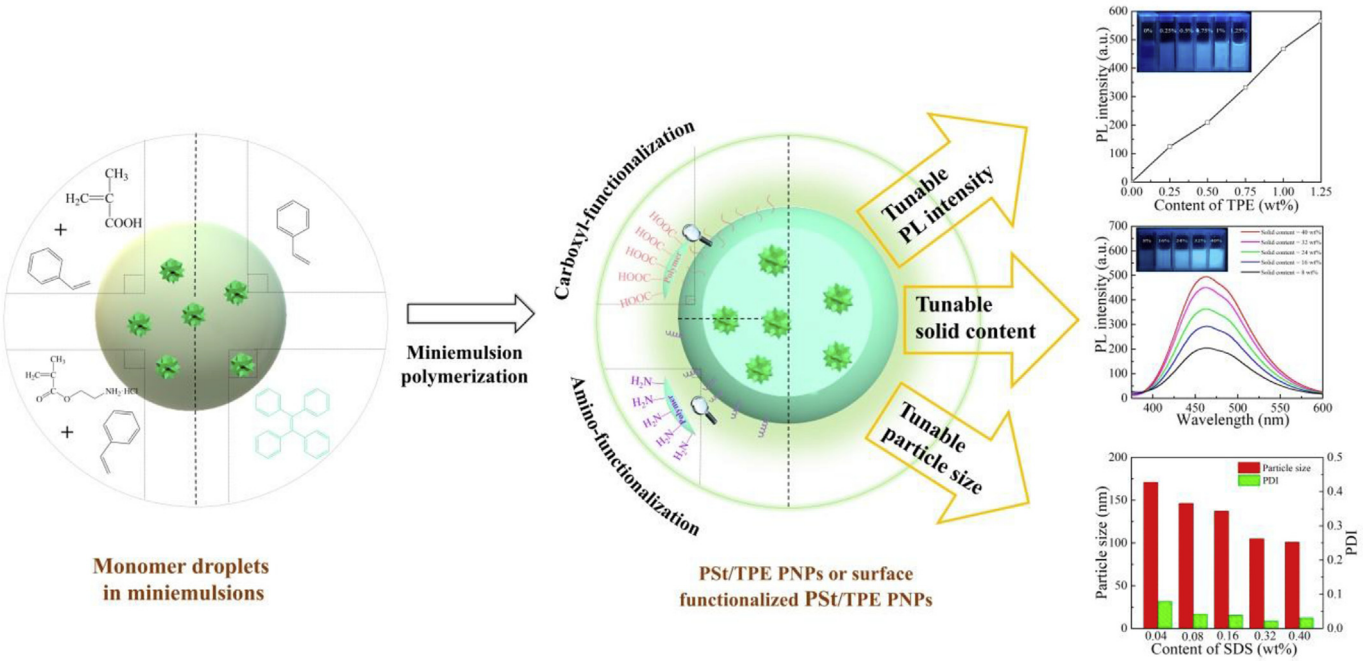

Scheme 1. Schematic representation of the preparation of PSt/TPE PNPs and surface functionalized PSt/TPE PNPs.

Table 1
Recipes for the prepared emulsions of PSt/TPE PNPs.

Sample	Oil phase			Water phase	
	St (g)	HD (g)	TPE (g)	SDS (g)	H_2O (g)
run 1	10	0.6	0.05	0.2	114
run 2	10	0.6	0	0.2	114
run 3	10	0.6	0.025	0.2	114
run 4	10	0.6	0.075	0.2	114
run 5	10	0.6	0.1	0.2	114
run 6	10	0.6	0.125	0.2	114
run 7	20	1.2	0.1	0.4	103
run 8	30	1.8	0.15	0.6	91
run 9	40	2.4	0.2	0.8	80
run 10	50	3	0.25	1.0	71
run 11	10	0.6	0.05	0.05	114
run 12	10	0.6	0.05	0.1	114
run 13	10	0.6	0.05	0.4	114
run 14	10	0.6	0.05	0.5	114

Table 2
Recipes for the prepared emulsions of carboxyl-functionalized PSt/TPE PNPs.

Sample	St (g)	MAA (g)	HD (g)	TPE (g)	SDS (g)	H_2O (g)	KPS (g)
run 15	9.9	0.1	0.6	0.1	0.2	114	0.05
run 16	9.75	0.25	0.6	0.1	0.2	114	0.05
run 17	9.5	0.5	0.6	0.1	0.2	114	0.05
run 18	9.25	0.75	0.6	0.1	0.2	114	0.05
run 19	9	1	0.6	0.1	0.2	114	0.05

Table 3
Recipes for the prepared emulsions of amino-functionalized PSt/TPE PNPs.

Sample	St (g)	AEMH (g)	HD (g)	TPE (g)	O-50 (g)	H_2O (g)	AIBN (g)
Run 20	1.000	0.000	0.06	0.01	0.2	12.5	0.02
Run 21	0.990	0.010	0.06	0.01	0.2	12.5	0.02
Run 22	0.975	0.025	0.06	0.01	0.2	12.5	0.02
Run 23	0.950	0.050	0.06	0.01	0.2	12.5	0.02
Run 24	0.925	0.075	0.06	0.01	0.2	12.5	0.02
Run 25	0.900	0.100	0.06	0.01	0.2	12.5	0.02

2.4. Determination of surface density of the carboxyl and amino groups on the AIE PNPs

Surface carboxyl- and amino-densities were determined through the conductometric back titration [46,47]. The dialyzed emulsion samples were used for the measurement. The protocol was as follows: 2 g of dialyzed emulsions was diluted with 70 g deionized water in a 200 mL beaker, and then the probes of pH meter (Mettler Toledo FE20) and conductivity meter (Mettler Toledo FE30) were placed in the diluted emulsion. An excess amount of aqueous NaOH solution (0.1 mol L^{-1}) was added to the diluted emulsions to reach a pH value of 10.5 ± 0.2. After 5-min stirring, the titration was started by adding 10 μL of the aqueous H_2SO_4 solution (0.1275 mol L^{-1}) in one shot each minute into the emulsion with a continuous stirring of 500 rpm. After each addition of aqueous H_2SO_4 solution, the equilibrated conductivities of emulsions were recorded. The conductometric back titration was finished when the conductivity of emulsions exceeded the value at time 0.

The molar amount of surface carboxyl or amino groups per gram of PNPs (S_b, mol·g^{-1}) was calculated through formula (1):

$$S_b = S_b' - S_0 \quad (1)$$

where S_b' (mol·g^{-1}) is the molar amount of surface carboxyl or amino groups per gram of surface functionalized PSt/TPE PNPs directly calculated through formula (2); the emulsion of un-functionalized PSt/TPE PNPs was used as the blank sample, and S_0 is the calculated molar amount of hypothetical surface carboxyl or amino groups per gram of un-functionalized PSt/TPE PNPs through formula (3).

$$S_b' = \frac{V_b \times C \times 2}{m \times W} \times 10^{-6} \quad (2)$$

$$S_0 = \frac{V_0 \times C \times 2}{m_0 \times W_0} \times 10^{-6} \quad (3)$$

where V_b is the volume of H_2SO_4 consumed by the carboxyl groups on the surface of PNPs or OH^- ions ionized by the amino groups of PNPs and H_2O (μL), V_0 is the volume of H_2SO_4 consumed by the PSt/TPE PNPs, C is the concentration of aqueous H_2SO_4 solution (mol·L^{-1}), m and m_0 are the masses of emulsion used for conductometric back titration (g), W and W_0 are the solid contents of dialyzed emulsion (wt%).

The number of carboxyl or amino groups per square nanometer was

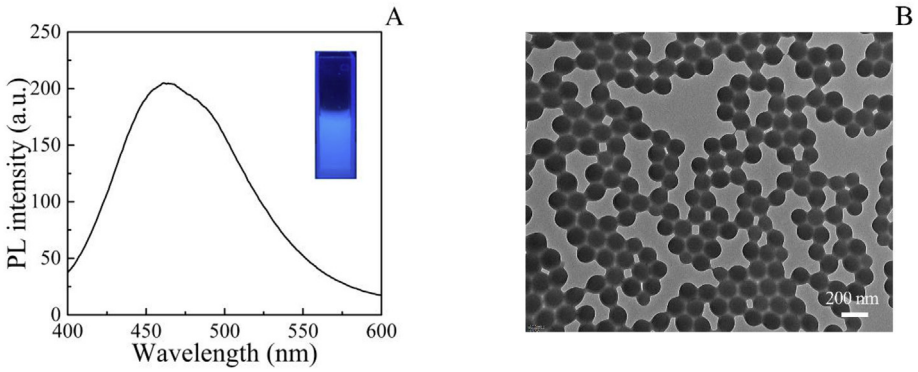

Fig. 1. (A) PL spectrum of PSt/TPE PNPs, (A, inset) photo of the PSt/TPE PNP emulsion under irradiation of UV light, and (B) TEM image of the PSt/TPE PNPs (Table 1, run 1).

calculated through formula (4).

$$[groups/nm^2] = \frac{N_A \times \rho \times S_b \times D_n}{6} \times 10^{-27} \quad (4)$$

where ρ is the density of PSt ($1.045 \times 10^6\ g\ m^{-3}$), D_n is the number-average particle size of PNPs determined by DLS, and N_A is Avogadro's constant ($6.022 \times 10^{23}\ mol^{-1}$).

2.5. Characterization

2.5.1. Measurement of monomer conversion

The final conversions of monomers were measured by gravimetric method. A certain amount of emulsions were dried at 70 °C for 24 h. Monomer conversions were calculated according to formula (5):

$$C = \frac{m_t \times \frac{m_2}{m_1} - m_s}{m_n} \times 100\% \quad (5)$$

in which m_n, m_t, m_s, m_1, and m_2 represent the feeding amount of monomers, the total feeding amount of materials, the amount of non-volatile components, the mass of the withdrawn emulsions, and the mass of the dried samples, respectively.

2.5.2. Transmission electron microscopy (TEM)

Particle morphology was observed by a JSM-1200EX transmission electron microscope (JEOL, Japan) with an acceleration voltage of 80 kV. The TEM sample was prepared as follows: a drop of emulsion was diluted with 2 mL distilled water; a drop of the diluted sample was placed on a 400-mesh carbon-coated copper grid and dried at room temperature.

2.5.3. Dynamic light scattering (DLS)

Z-average particle sizes, number-average particle sizes, and polydispersities (PDIs) of the PSt/TPE PNPs and surface functionalized PSt/TPE PNPs were measured by DLS (Zetasizer Nanoseries) at 25 °C under a scattering angle of 90°. A drop of emulsion was diluted with 2 mL of distilled water. Particle sizes were given as the average of three measurements.

2.5.4. Fluorescence spectroscopy

Five microliter of aqueous PSt/TPE PNP or surface functionalized PSt/TPE PNP emulsion was diluted with 2 mL distilled water. The PL spectra of the diluted AIE PNP emulsions were recorded on a Hitachi F-4600 spectrofluorometer in a spectral range of 350–600 nm at the excitation wavelength of 330 nm.

2.5.5. Zeta potential measurement

Zeta potential of PSt/TPE PNPs, surface carboxyl- and amino-functionalized PSt/TPE PNPs were measured at 25 °C on a Zetasizer nanoseries potentiometer. The preparation of samples was as follows: The PSt/TPE PNP emulsions (run 5) and carboxyl-functionalized PSt/TPE PNP emulsions were diluted with an aqueous solution of KCl ($10^{-3}\ mol\ L^{-1}$, pH = 8.0 ± 0.1) to a mass fraction of ~0.125 wt%; The PSt/TPE PNPs emulsions (run 20) and amino-functionalized PSt/TPE PNP emulsions were diluted with an aqueous solution of KCl ($10^{-3}\ mol\ L^{-1}$, pH = 3.0 ± 0.1) to a mass fraction of ~0.125 wt%.

2.5.6. Fourier transformation infrared spectroscopy (FTIR)

FTIR spectra of the PSt/TPE PNPs, surface carboxyl- and amino-functionalized PSt/TPE PNPs were recorded on a Vertex 70 Fourier transformation infrared spectrometer. The powder samples were mixed with KBr and pressed to form a sample disk.

3. Results and discussion

3.1. Synthesis of PSt/TPE PNPs through miniemulsion polymerization

In this work, PSt/TPE PNPs were prepared through polymerization of TPE-containing monomer miniemulsions (Scheme 1). The TPE molecules were physically embedded in the PSt matrix. Under room temperature, the matrix polymer was under its glassy state, and thus the polymer chain segments were frozen. As a result, the doped TPE molecules in the PNPs could emit strong fluorescence due to the highly restricted intramolecular motion (Fig. 1A, inset). Quantitatively, the spectroscopic result showed that a strong PL peak in the spectral range of 400–600 nm that centered at ~460 nm appeared in the PL spectrum of PSt/TPE PNPs (Fig. 1A).

The PSt/TPE PNPs displayed a well-defined spherical morphology (Fig. 1B). The Z-average particle size and PDI of PSt/TPE PNPs were 137.4 and 0.039, respectively, displaying a narrow particle size distribution.

3.2. Tuning the brightness of PSt/TPE PNPs

As the glass transition temperature of PSt (97 °C [48]) is much higher than that of room temperature, the TPE molecules are frozen in the glassy PSt matrix of PSt/TPE PNPs. Therefore, both the aggregated and molecularly-dispersed TPE molecules can emit fluorescence due to the restricted intramolecular rotation. Moreover, different from conventional ACQ dyes, the concentration-induced aggregation of TPE does not lead to its fluorescence quenching [12]. Therefore, the brightness of AIE PNPs may increase with the increase of the TPE content. As shown in Fig. 2A, the PSt/TPE PNPs with various TPE contents exhibit the TPE characteristic PL peak at ~460 nm. Promisingly, the peak PL intensity of the PSt/TPE PNPs increased linearly with the increase of the TPE content. It means that the brightness of the AIE PNPs can be accurately tuned by the TPE content. This attribute of PSt/TPE PNPs could be reasonably ascribed to the unique AIE mechanism of

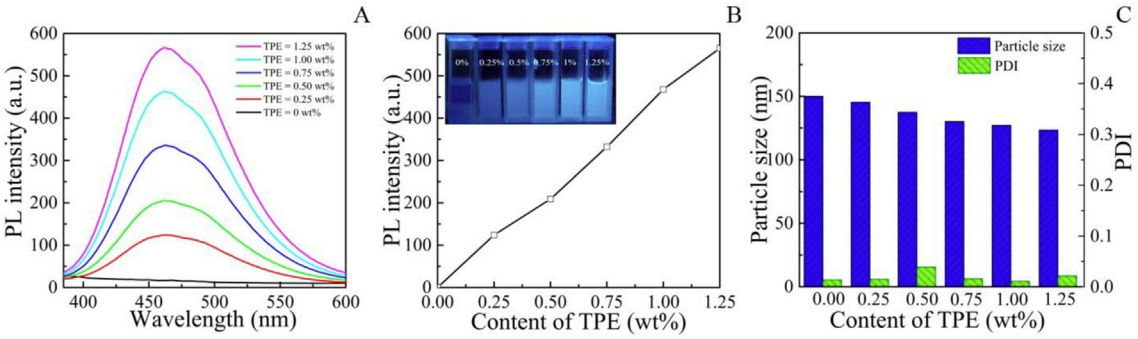

Fig. 2. (A) PL spectra of the PSt/TPE PNPs with various TPE contents. (B) Relationship between the peak intensity and the TPE content and (B inset) photo of the PSt/TPE PNP emulsions with various TPE contents under irradiation of UV light. (C) Z-average particle sizes and PDIs of the PSt/TPE PNPs with various TPE contents (Table 1, runs 1–6).

TPE.

It should be pointed out that the particle size of PSt/TPE PNPs slightly decreased with the increase of the TPE content (Fig. 2C). This decrement could be ascribed to the high hydrophobicity of TPE, which may function as a hydrophobe to improve the stability of monomer droplets. All the PSt/TPE PNPs with various TPE contents had a very low PDI values, indicating the good uniformity of the particles.

3.3. Tuning the solid content of PSt/TPE PNP emulsions

As mentioned in the introduction, miniemulsion polymerization technique holds high promise to prepare high solid content emulsions [31,32]. In this work, the PSt/TPE PNP emulsions with a solid content of 8 wt% to 40 wt% were prepared. As shown in Fig. 3A, the particle size of PSt/TPE PNPs was not affected by the solid content in the range of 8–32 wt%. Further increase of the solid content to 40 wt%, the particle size of PSt/TPE NPs slightly increased. This could be ascribed to the high viscosity of the crude emulsion with 40 wt% of monomers, leading to the increased dispersion difficulty in the preparation of monomer miniemulsion by sonication. Promisingly, the PSt/TPE PNPs in the emulsions with various solid contents had low PDI values. It means that the solid content of emulsion does not show obvious influence on the particle size distribution of AIE PNPs.

The visual observation showed that the higher the solid content of PSt/TPE PNP emulsion was, the brighter the PL emission was (Fig. 3B inset). For quantitative evaluation, the same amount of emulsions with various solid contents was withdrawn for PL spectroscopic measurements, and the results are shown in Fig. 3B. The peak PL intensity of the PSt/TPE PNPs almost linearly increased with the increase of the solid content (Fig. 3C). This could be reasonably ascribed to the increase of the TPE concentration along with the solid content. The PSt/TPE PNP emulsions with various solid contents were diluted to the same NP concentration prior to the PL spectroscopic measurements, and the corresponding PL spectra are shown in Fig. 3D. As the TPE content in the PNPs was kept fixed, the emulsion with the same PNP concentration contained the same amount of incorporated TPE. As expected, the peak PL intensity of PSt/TPE PNPs synthesized in the systems with various solid contents remained almost unchanged (Fig. 3E). This result indicated that the brightness of PSt/TPE PNPs synthesized in the systems with various solid contents only depended on the incorporated content of TPE, and therefore they displayed very similar emission behaviors. In other words, the PSt/TPE NPs with similar emission property can be easily synthesized through our proposed miniemulsion polymerization at various solid content levels, and more promisingly, they can be efficiently synthesized at a high solid content level.

3.4. Tuning the particle size of PSt/TPE PNPs

For biological applications, the particle size of PNPs is an important index that may significantly impact the uptake efficiency and imaging effect of cells [14]. For miniemulsion polymerization systems, the particle size of PNPs may be conveniently tuned by the surfactant amount [49]. As shown in Fig. 4A, the particle size of PSt/TPE PNPs could be tuned from 146 nm to 105 nm by increasing the SDS amount from 0.04 wt% to 0.4 wt% relative to water.

The PL spectra of the PSt/TPE PNPs with varied content of SDS are shown in Fig. 4B. All the samples displayed an obvious emission peak at ~460 nm. The peak PL intensity slightly increased with the increase of SDS content. This increment could be ascribed to the less light scattering intensity of the PSt/TPE PNPs with a relatively smaller particle size (higher SDS content).

3.5. Surface functionalization of PSt/TPE PNPs

AIE PNPs with targeted functional groups have greater advantages in the specific recognition of cells and tissues [1,50]. However, there is no reactive functional groups on the surface of PSt/TPE PNPs, which cannot directly achieve specific modification of target groups. Thanks to the high hydrophilicity of MAA or AEMH monomeric units, these surface active monomeric units are thermodynamically inclined to partition onto the surface of PNPs [47]. It has been reported that the surface carboxyl- or amino-functionalization of hydrophobic PNPs could be realized through introducing a small amount of carboxyl- or amino-containing hydrophilic comonomers into emulsion or miniemulsion polymerization systems [22,43,44]. In this work, MAA and AEMH were added to the miniemulsion polymerization systems to prepare surface carboxyl- and amino-functionalized PSt/TPE PNPs through the copolymerization of St and MAA or AEMH, respectively.

3.5.1. Surface carboxyl-functionalization of PSt/TPE PNPs

As shown in Fig. 5A, the miniemulsion copolymerization of St and MAA could be efficiently carried out, and all the reaction systems could reach a high final overall monomer conversion (> 85%). Fig. 5B shows the FTIR spectra of PSt/TPE PNPs and poly(St-*co*-MAA)/TPE PNPs with various MAA contents. In comparison to PSt/TPE PNPs (Fig. 5B, curve a), additional characteristic bands in the spectral range of 1650–1700 and 3300–3500 cm^{-1} appeared in all the spectra of poly(St-*co*-MAA)/TPE NPs with various MAA contents (Fig. 5, curves b–d), which could be assigned to the stretching vibration of C=O and –OH groups originated from the carboxyl groups of MAA units, respectively. The FTIR results clearly indicated that the successful introduction of MAA units to the PSt/TPE NPs.

Although the FTIR results showed that MAA has been successfully introduced into the PSt/TPE PNPs, only the carboxyl groups on the surface of PNPs can be used for the further functional modification. Therefore, the density of carboxyl groups on the surface of the poly(St-*co*-MAA)/TPE PNPs with various MAA contents was characterized by the method of conductometric back titration, and the corresponding

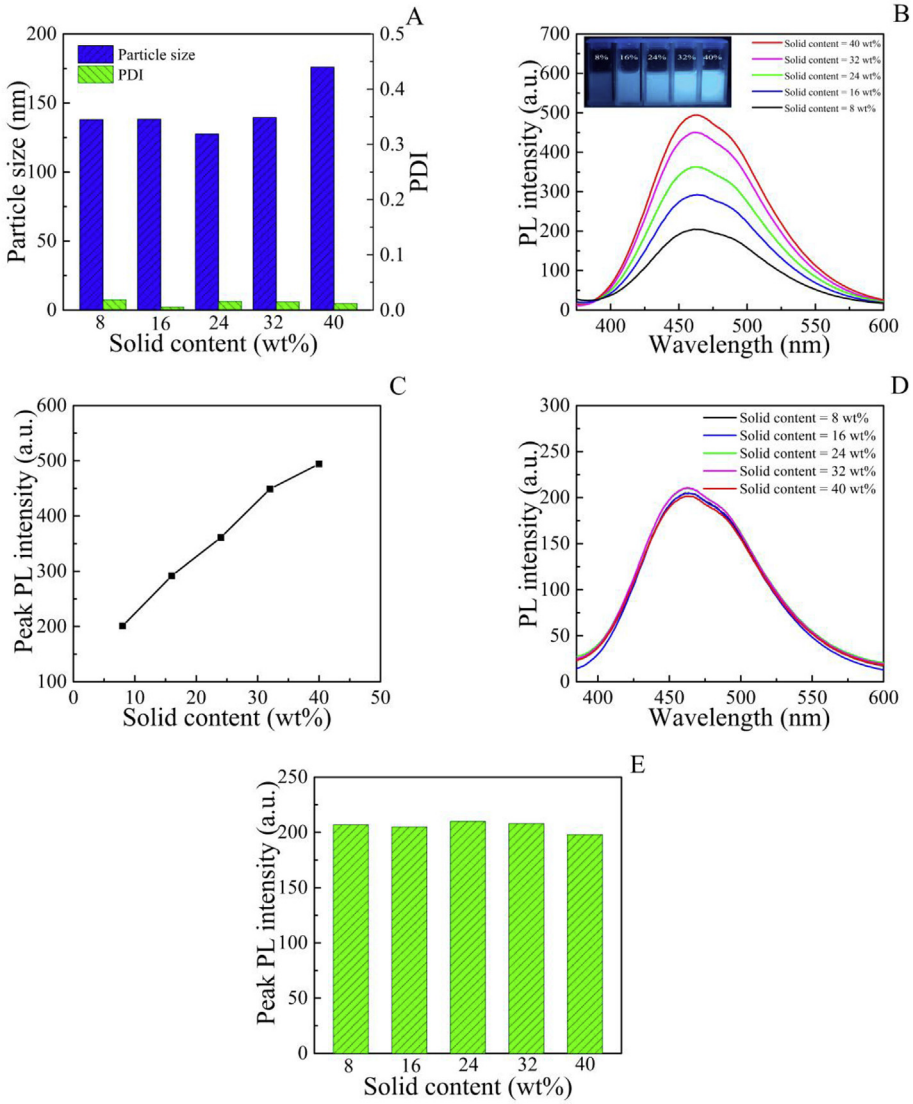

Fig. 3. (A) Z-average particle sizes and PDIs of the PSt/TPE PNPs with various solid contents. (B) PL spectra and (C) peak PL intensity of the PSt/TPE PNP emulsions with various solid contents (5 μL of original emulsions with solid contents of 8 wt%, 16 wt %, 24 wt%, 32 wt%, and 40 wt% were diluted with 2 mL of water, respectively). (B, inset) Photos of the PSt/TPE PNP emulsions with various solid contents under irradiation of UV light. (D) PL spectra and (E) peak PL intensity of the PSt/TPE PNP emulsions with various solid contents at the same PNP concentration (5 μL of original emulsions with solid contents of 8 wt%, 16 wt%, 24 wt%, 32 wt%, and 40 wt% were diluted with 2 mL, 4 mL, 6 mL, 8 mL, and 10 mL of water, respectively, to achieve the same PNP concentration.) (Table 1, runs 1, and 7–10).

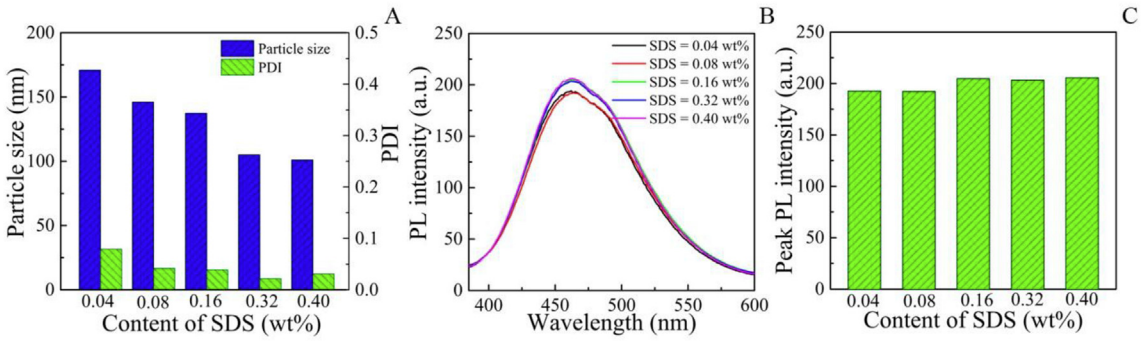

Fig. 4. (A) Z-average particle sizes and PDIs and (B) PL spectra of the PSt/TPE PNPs synthesized in the miniemulsion system with various SDS contents. (C) Relationship between the peak intensity and the content of SDS (Table 1, runs 1, and 11–14).

conductometric titration curves are shown in Figs. 6A and S1. As shown in Fig. 6A, the conductometric titration curve contained four stages: Stage I corresponds to the neutralization of NaOH with H_2SO_4, Stage II represents the neutralization of surface-bound carboxylic ions, and Stages III and IV correspond to the neutralization of free carboxylic ions in the aqueous phase and excess H_2SO_4, respectively.

The variables including the number-average particle size of AIE PNPs, the solid content of the dialyzed emulsion, and the volume of H_2SO_4 solution consumed by the surface-bound carboxylic ions are listed in Table S1. The densities of carboxyl groups on the particle surface were calculated according to formula (1)–(4), and the results are shown in Fig. 6B. The density of the surface carboxyl groups almost linearly increased with the increase of the MAA content. It means that the amount of surface carboxyl groups can be conveniently tuned by the MAA content in our experimental range.

The Z-average particle sizes and PDIs of the surface carboxyl-

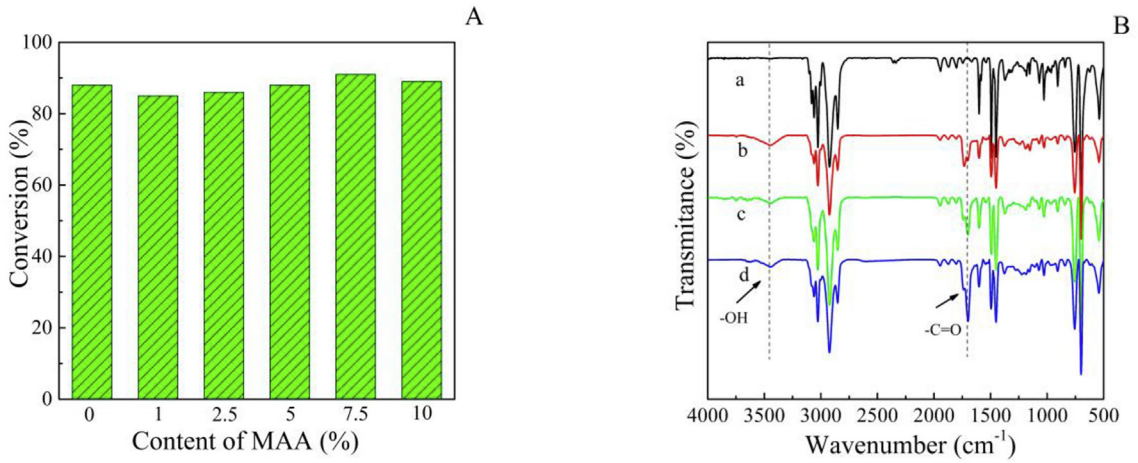

Fig. 5. (A) Final overall monomer conversions of the systems with various MAA contents. (B) FTIR spectra of PSt/TPE and poly(St-*co*-MAA)/TPE PNPs with various contents of MAA (a, PSt/TPE PNPs; b, poly(St-*co*-1% MAA)/TPE PNPs; c, poly(St-*co*-5% MAA)/TPE PNPs; d, poly(St-*co*-10% MAA)/TPE PNPs) (Tables 1 and 2, runs 5, and 15–19).

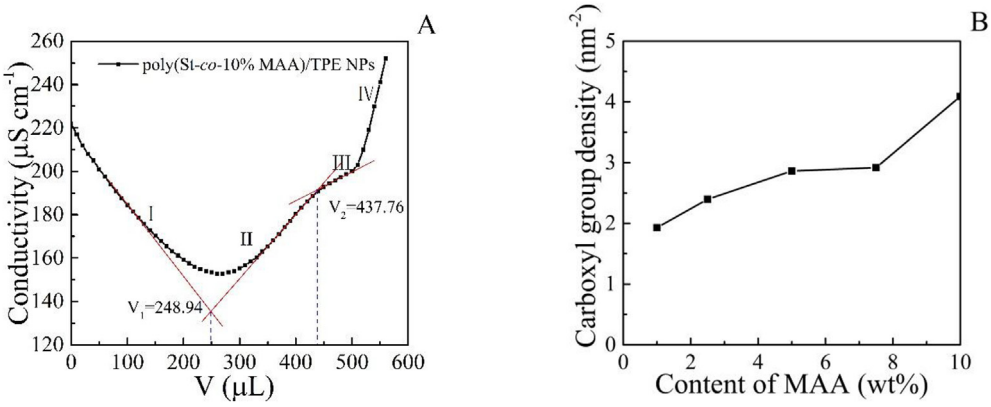

Fig. 6. (A) Conductometric titration curve of the poly(St-*co*-10%MAA)/TPE PNPs. (B) Relationship between the number of surface carboxyl groups per unit nm^2 and MAA content (Table 2, runs 15–19).

functionalized PSt/TPE PNPs with various MAA contents were measured by DLS, and the results are shown in Fig. 7A. In the range of 0–10 wt% of MAA, the particle size of the poly(St-*co*-MAA)/TPE PNPs varied in the range of 105–130 nm and did not show a clear dependence on the weight content of MAA. All the surface carboxyl-functionalized PSt/TPE PNPs had a low PDI value, displaying a narrow particle size distribution. All the poly(St-*co*-MAA)/TPE PNPs displayed a very negative zeta potential values due to the surface carboxyl-functionalization (Fig. 7B). It should be pointed out that the residue groups of initiator (KPS) also partially contributed to the surface negative charge of AIE PNPs.

The PL spectra of the carboxyl-functionalized AIE PNPs with various MAA contents are shown in Fig. 7C. Regardless of the MAA content, the PL spectra of the poly(St-*co*-MAA)/TPE PNPs did not show any obvious difference, and had very similar peak PL intensity (Fig. 7D). All the results illustrated that the surface carboxyl-functionalization through miniemulsion copolymerization of St and MAA only had minor influence on the particle size, particle size distribution, and PL behavior of poly(St-*co*-MAA)/TPE PNPs.

3.5.2. Surface amino-functionalization of PSt/TPE PNPs

Amino-functionalized PSt/TPE PNPs were prepared through miniemulsion copolymerization of St and AEMH. As shown in Fig. 8A, the overall monomer conversions of the polymerization systems with various contents of AEMH reached above 82%, indicating that the copolymerization of St and AEMH was very efficient. Fig. 8B shows the FTIR spectra of PSt/TPE PNPs and poly(St-*co*-AEMH)/TPE PNPs with various AEMH contents. In comparison to PSt/TPE PNPs (Fig. 8B, curve a), new peaks appeared at 1730, 1100, and 1380 cm^{-1}, which correspond to the stretching vibration of C=O, stretching vibration of C–O, and stretching vibration C–N bond from AEMH, respectively [51]. In addition, the characteristic bands in the spectral range of 3400–3700 cm^{-1} appeared in all the spectra of poly(St-*co*-AEMH)/TPE PNPs with various AEMH contents (Fig. 8B, curves b–d), which could be assigned to the amino groups introduced by AEMH [51]. The FTIR results clearly indicated that the successful introduction of AEMH units to the PSt/TPE PNPs.

Similarly, the surface amino density of poly(St-*co*-AEMH)/TPE PNPs was determined by conductometric back titration, and the conductometric titration curves are shown in Figs. 9A and S2. The variables for calculating the number of surface amino groups of poly(St-*co*-AEMH)/TPE PNPs, including the number-average particle size of PNPs, solid content of emulsion, and volume of H_2SO_4 solution consumed by surface-bound amino groups are listed in Table S2. As shown in Fig. 9B, the surface density of amino groups displayed a positive correlation with the content of AEMH, similar to the surface carboxyl functionalization of PSt/TPE PNPs.

Fig. 10A shows the Z-average particle sizes and PDI values of the PSt/TPE PNPs with various AEMH contents. Although addition of AEMH induced a slight increment in the particle size and PDI of PSt/TPE PNPs, the particle sizes of the PNPs could still be well controlled in the range of 1–10 wt% of AEMH content, and they only varied in the

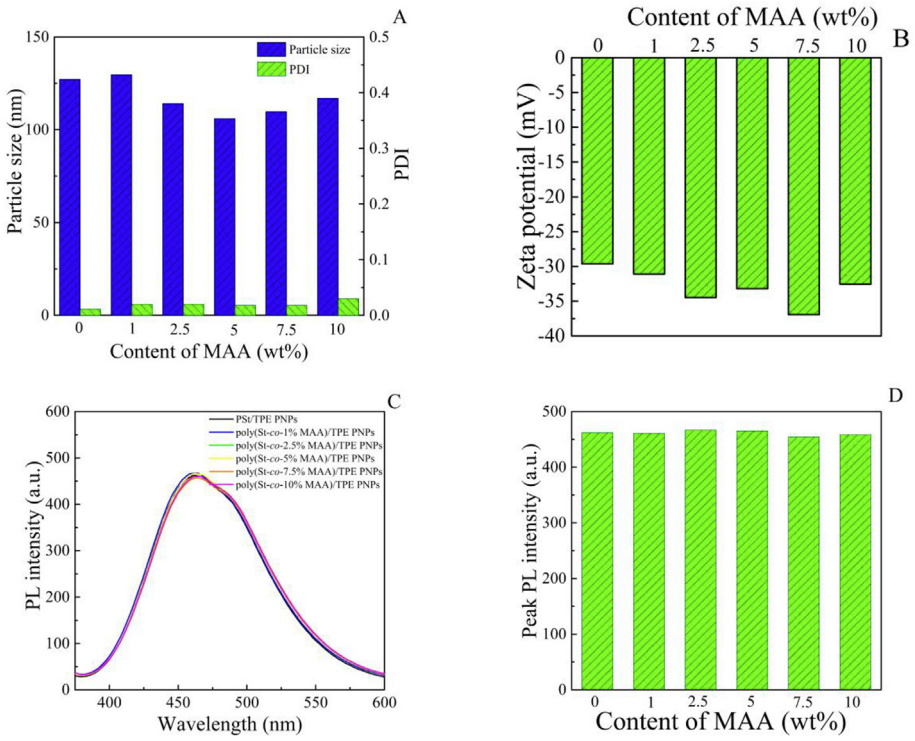

Fig. 7. (A) Z-average particle sizes and PDIs and (B) zeta potential values of the carboxyl-functionalized PSt/TPE PNPs with various MAA contents. (C) PL spectra and (D) peak PL intensity of PSt/TPE PNPs with various MAA contents (Tables 1 and 2, runs 5, and 15–19).

range of 80–95 nm. Moreover, the amino-functionalized PSt/TPE PNPs still displayed a relatively low PDI value, indicative of a narrow particle size distribution. Due to the introduction of various amounts of amino groups to the surface of PSt/TPE PNPs, the zeta potential values increased with the increase of the AEMH content. It confirmed the existence of amino functional groups on the surface of AIE PNPs.

Furthermore, like the carboxyl-functionalized AIE PNPs, the amino-functionalized AIE PNPs exhibited obvious PL emission at ~460 nm (Fig. 10C). Surface modification of AEMH did not show obvious influence on the PL emission property of the AIE PNPs, and all the PNPs displayed a similar peak PL intensity (Fig. 10D). It means that the PSt/TPE PNPs could be surface-modified by AEMH without interfering the PL emission of the incorporated TPE molecules.

4. Conclusions

In summary, un-functionalized, surface carboxyl-functionalized or surface amino-functionalized PSt/TPE PNPs were facilely synthesized by encapsulating TPE within a polymer matrix via miniemulsion polymerization of St or copolymerization of St with various functional monomers. The synthesized AIE PNPs displayed a well-defined spherical morphology and narrow particle size distribution. The PL intensity of AIE PNPs could be accurately tuned by changing the TPE content. The particle size of AIE PNPs could be tuned from 105 to 146 nm by varying the SDS content. Promisingly, the AIE PNPs with similar emission property were efficiently synthesized at various levels of solid content, especially at a very high solid content (40 wt%). The surface of AIE PNPs was functionalized by carboxyl and amino groups through

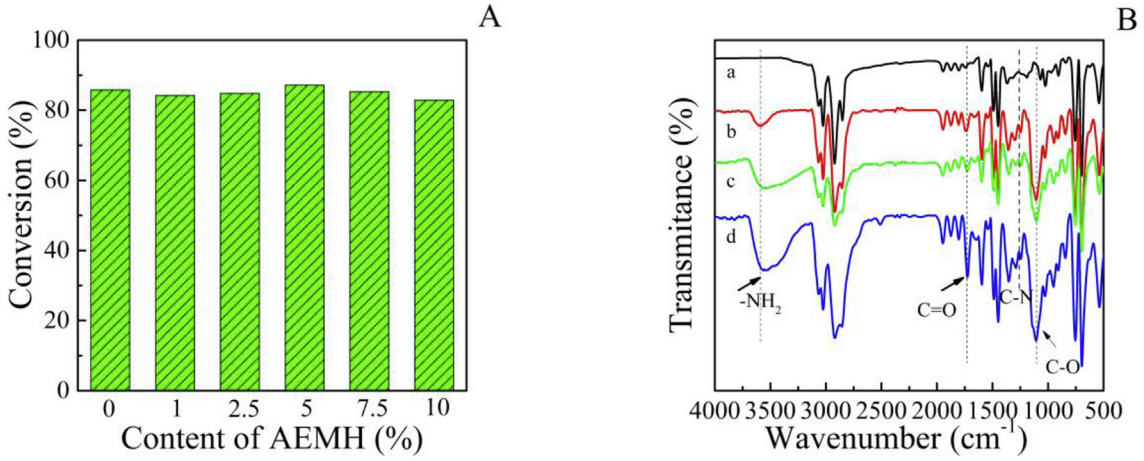

Fig. 8. (A) Final overall monomer conversions of the systems with various AEMH contents. (B) FTIR spectra of PSt/TPE and poly(St-*co*-AEMH)/TPE PNPs with various contents of AEMH (a, PSt/TPE PNPs; b, poly(St-*co*-1%AEMH)/TPE PNPs; c, poly(St-*co*-5%AEMH)/TPE PNPs; d, poly(St-*co*-10%AEMH)/TPE PNPs) (Table 3, runs 20–25).

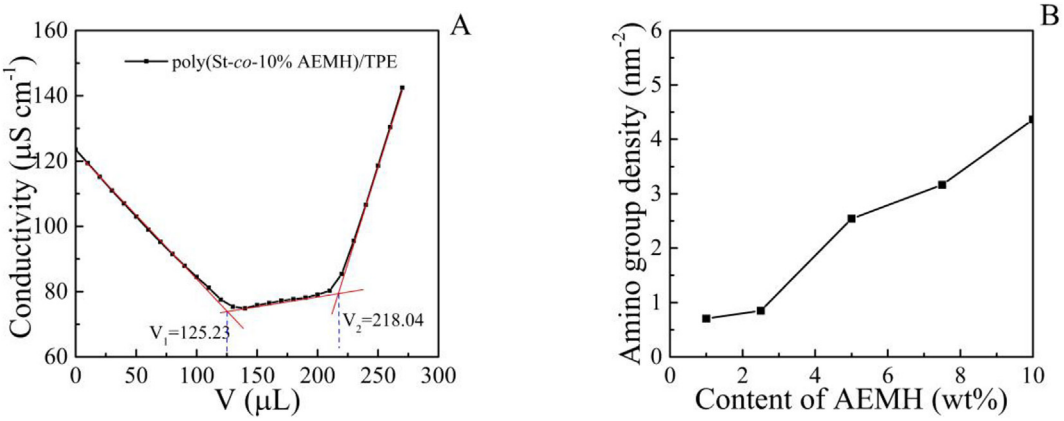

Fig. 9. (A) Conductometric titration curve of the poly(St-*co*-10%AEMH)/TPE PNPs. (B) Relationship between the number of surface amino groups per unit nm^2 and AEMH content (Table 3, runs 20–25).

introduction of MAA and AEMH, respectively. The surface density of functional groups positively correlated to the content of functional monomers, and therefore the surface modification could be tuned by the content of functional monomer. Although the surface functionalization markedly affected the surface properties of AIE PNPs, like charge and reactivity, it only displayed a minor influence on the PL behavior of AIE PNPs. The miniemulsion polymerization technique proposed in this work holds high promise to efficiently synthesize versatile AIE PNPs at a high level of solid content with tunable brightness, versatile surface functionalization, and controllable particle properties.

Conflicts of interest

The authors declare no conflict of interest.

Acknowledgements

Financial supports from the National Natural Science Foundation of China project (51573168 and U1609205), the Zhejiang Provincial Natural Science Foundation (LY16E030006 and LZ18E030002), the Science Foundation of Zhejiang Sci-Tech University (14012208-Y), the

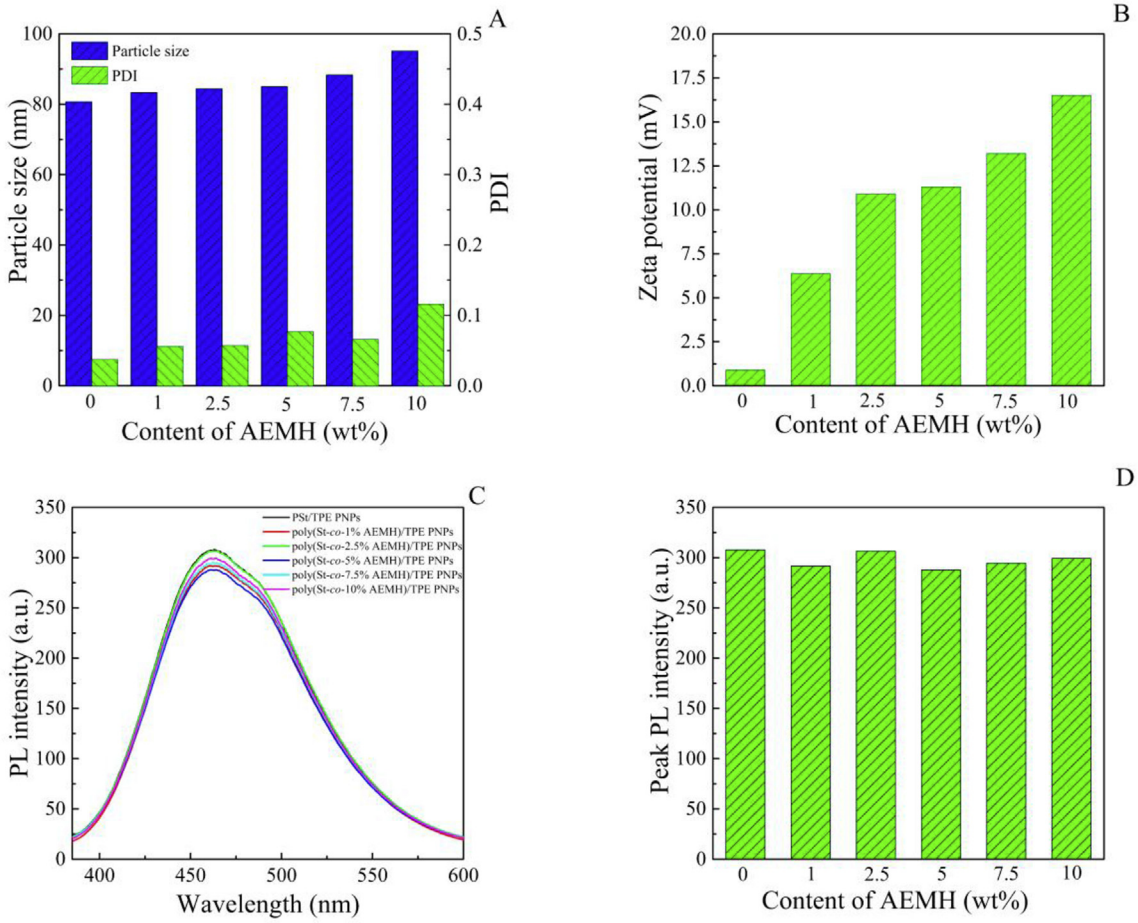

Fig. 10. (A) Z-average particle sizes and PDIs and (B) zeta potential values of the amino-functionalized PSt/TPE PNPs with various AEMH contents. (C) PL spectra and (D) peak PL intensity of PSt/TPE PNPs and poly(St-*co*-AEMH)/TPE PNPs with various AEMH contents (Table 3, runs 20–25).

Excellent Young Researchers Foundation (CETT2015001) of Zhejiang Provincial Top Key Academic Discipline of Chemical Engineering and Technology, Zhejiang Province's Xinmiao Talent Plan (2017R406020 and 2017R406022) and National Undergraduate Training Programs for Innovation and Entrepreneurship of China (201710338021) are gratefully acknowledged.

Appendix A. Supplementary data

Supplementary data to this article can be found online at https://doi.org/10.1016/j.dyepig.2018.12.018.

References

[1] Reisch A, Klymchenko AS. Fluorescent polymer nanoparticles based on dyes: seeking brighter tools for bioimaging. Small 2016;12:1968–92.
[2] Chen MJ, Yin MZ. Design and development of fluorescent nanostructuresfor bioimaging. Prog Polym Sci 2014;39:365–95.
[3] Ding D, Li K, Liu B, Tang BZ. Bioprobes based on AIE fluorogens. Acc Chem Res 2013;46:2441–53.
[4] Gu XG, Kwok RTK, Lam JWY, Tang BZ. AIEgens for biological process monitoring and disease theranostics. Biomaterials 2017;146:115–35.
[5] Liu XC, Nian L, Gao K, Zhang LJ, Qing LC, Wang Z, et al. Low band gap conjugated polymers combining siloxane-terminated side chains and alkyl side chains: side-chain engineering achieving a large active layer processing window for PCE > 10% in polymer solar cells. J Mater Chem 2017;5:17619–31.
[6] Gao K, Li LS, Lai TQ, Xiao LG, Huang Y, Huang F, et al. Deep absorbing porphyrin small molecule for high-performance organic solar cells with very low energy losses. J Am Chem Soc 2015;137:7282–5.
[7] Gao K, Zhu ZL, Xu B, Jo SB, Kan YY, Peng XB, et al. Highly efficient porphyrin-based OPV/perovskite hybrid solar cells with extended photoresponse and high fill factor. Adv Mater 2017;29. 1703980.
[8] Gao K, Miao JS, Xiao LG, Deng WY, Kan YY, Liang TX, et al. Multi-length-scale morphologies driven by mixed additives in porphyrin-based organic photovoltaics. Adv Mater 2016;28:4727–33.
[9] Gao K, Xu B, Hong CS, Shi XL, Liu HB, Li XS, et al. Di-spiro-based hole-transporting materials for highly effcient perovskite solar cells. Adv Energy Mater 2018;8. 1800809.
[10] Zhang XY, Wang K, Liu MY, Tao L, Chen YW, Wei Y. Polymeric AIE-based nanoprobes for biomedical applications: recent advances and perspectives. Nanoscale 2015;7:11486–508.
[11] Hong YN, Lam JWY, Tang BZ. Aggregation-induced emission: phenomenon, mechanism and applications. Chem Commun 2009:4332–53.
[12] Hong YN, Lam JWY, Tang BZ. Aggregation-induced emission. Chem Soc Rev 2011;40:5361–88.
[13] Zhao ZJ, He BR, Tang BZ. Aggregation-induced emission of siloles. Chem Sci 2015;6:5347–65.
[14] Chen SJ, Wang H, Hong YN, Tang BZ. Fabrication of fluorescent nanoparticles based on AIE luminogens (AIE dots) and their applications in bioimaging. Mater Horiz 2016;3:283–93.
[15] Wan Q, Huang Q, Liu MY, Xu DZ, Huang HY, Zhang XY, et al. Aggregation-induced emission active luminescent polymeric nanoparticles: non-covalent fabrication methodologies and biomedical applications. Appl Mater Today 2017;9:145–60.
[16] Qin W, Ding D, Liu JZ, Yuan WZ, Hu Y, Liu B, et al. Biocompatible nanoparticles with aggregation-induced emission characteristics as far-red/near-infrared fluorescent bioprobes for in vitro and in vivo imaging applications. Adv Funct Mater 2012;22:771–9.
[17] Zhang XQ, Liu MY, Yang B, Zhang XY, Chi ZG, Liu SW, et al. Cross-linkable aggregation induced emission dye based red fluorescent organic nanoparticles and their cell imaging applications. Polym Chem 2013;4:5060–4.
[18] Li HY, Zhang XQ, Zhang XY, Yang B, Yang Y, Wei Y. Ultra-stable biocompatible cross-linked fluorescent polymeric nanoparticles using AIE chain transfer agent. Polym Chem 2014;5:3758–62.
[19] Huang HY, Xu DZ, Liu MY, Jiang RM, Mao LC, Huang Q, et al. Direct encapsulation of AIE-active dye with β-cyclodextrin terminated polymers: self-assembly and biological imaging. Mater Sci Eng C 2017;78:862–7.
[20] Bao YY, Guégain E, Nicolas V, Nicolas J. Fluorescent polymer prodrug nanoparticles with aggregation-induced emission (AIE) properties from nitroxide-mediated polymerization. Chem Commun 2017;53:4489–92.
[21] Li X, Li CP, Wang S, Dong H, Ma X, Cao DR. Synthesis and properties of photochromic spirooxazine with aggregation-induced emission fluorophores polymeric nanoparticles. Dyes Pigments 2017;142:481–90.
[22] Liu MY, Zhang XQ, Yang B, Deng FJ, Li Z, Wei JC, et al. Water dispersible, non-cytotoxic, cross-linked luminescent AIE dots:Facile preparation and bioimaging applications. Appl Surf Sci 2014;322:155–61.
[23] Zhang XY, Zhang XQ, Yang B, Liu MY, Liu WY, Chen YW, et al. Fabrication of aggregation induced emission dye-based fluorescent organic nanoparticles via emulsion polymerization and their cell imaging applications. Polym Chem 2014;5:399–404.
[24] Wan Q, Jiang RM, Mao LC, Xu DZ, Zeng GJ, Shi YG, et al. A powerful "one-pot" tool for fabrication of AIE-active luminescent organic nanoparticles through the combination of RAFT polymerization and multicomponent reactions. Mater Chem Front 2017;1:1051–8.
[25] Long Z, Liu MY, Mao LC, Zeng GJ, Wan Q, Xu DZ, et al. Rapid preparation of branched and degradable AIE-active fluorescent organic nanoparticles via formation of dynamic phenyl borate bond. Colloids Surf, B 2017;150:114–20.
[26] Jiang RM, Liu MY, Huang HY, Mao LC, Huang Q, Wen YQ, et al. Facile fabrication of organic dyed polymer nanoparticles with aggregation-induced emission using an ultrasound-assisted multicomponent reaction and their biological imaging. J Colloid Interface Sci 2018;519:137–44.
[27] Zeng GJ, Liu MY, Jiang RM, Huang Q, Huang L, Wan Q, et al. Fabrication of water dispersible and biocompatible AIE-active fluorescent polymeric nanoparticles through a "one-pot" Mannich reaction. Polym Chem 2017;8:4746–51.
[28] Jiang RM, Liu MY, Huang Q, Huang HY, Wan Q, Wen YQ, et al. Fabrication of multifunctional fluorescent organic nanoparticles with AIE feature through photo-initiated RAFT polymerization. Polym Chem 2017;8:7390–9.
[29] Jiang RM, Liu MY, Huang HY, Mao LC, Huang Q, Wen YQ, et al. Fabrication of AIE-active fluorescent polymeric nanoparticles with red emission through a facile catalyst-free amino-yne click polymerization. Dyes Pigments 2018;151:123–9.
[30] Guyot A, Chu F, Schneider M, Graillat C, Mckenna TF. High solid content latexes. Prog Polym Sci 2002;27:1573–615.
[31] Leiza JR, Sudol ED, El-Aasser MS. Preparation of high solids content poly(*n*-butyl acrylate) latexes through miniemulsion polymerization. J Appl Polym Sci 1997;64:1797–809.
[32] Do Amaral M, Asua JM. Synthesis of large, high-solid-content latexes by miniemulsion polymerization. J Polym Sci, Part A: Polym Chem 2004;42:4222–7.
[33] Ouzineb K, Graillat C, McKenna TF. High-solid-content emulsions. V. Applications of miniemulsions to high solids and viscosity control. J Appl Polym Sci 2005;97:745–52.
[34] Ballard N, Aguirre M, Simula A, Leiza JR, van Es S, Asua JM. High solids content nitroxide mediated miniemulsion polymerization of *n*-butyl methacrylate. Polym Chem 2017;8:1628–35.
[35] Rodríguez R, Barandiaran MJ, Asua JM. Particle nucleation in high solids miniemulsion polymerization. Macromolecules 2007;40:5735–42.
[36] González-Matheus K, Leal GP, Tollan C, Asua JM. High solids Pickering miniemulsion polymerization. Polymer 2013;54:6314–20.
[37] Ronco LI, Minari RJ, PJMC G, Meira GR, Gugliotta LM. Toughened polystyrene nanoparticles through high-solids miniemulsion polymerization. Chem Eng J 2015;263:231–8.
[38] Diaconu G, Paulis M, Leiza JR. High solids content waterborne acrylic/montmorillonite nanocomposites by miniemulsion polymerization. Macromol React Eng 2008;2:80–9.
[39] Landfester K. Miniemulsion polymerization and the structure of polymer and hybrid nanoparticles. Angew Chem Int Ed 2009;48:4488–507.
[40] Qi DM, Cao ZH, Ziener U. Recent advances in the preparation of hybrid nanoparticles in miniemulsions. Adv Colloid Interface Sci 2014;211:47–62.
[41] Cao ZH, Xu C, Liang LH, Zhao ZJ, Chen B, Chen ZJ, et al. A green miniemulsion-based synthesis of polymeric aggregation-induced emission nanoparticles. Polym Chem 2015;6:6378–85.
[42] Cao ZH, Liang XQ, Chen HN, Gao M, Zhao ZJ, Chen XL, et al. Bright and biocompatible AIE polymeric nanoparticles prepared from miniemulsion for fluorescence cell imaging. Polym Chem 2016;7:5571–8.
[43] Holzapfel V, Musyanovych A, Landfester K, Lorenz MR, Mailaender V. Preparation of fluorescent carboxyl and amino functionalized polystyrene particles by miniemulsion polymerization as markers for cells. Macromol Chem Phys 2005;206:2440–9.
[44] Musyanovych A, Rossmanith R, Tontsch C, Landfester K. Effect of hydrophilic comonomer and surfactant type on the colloidal stability and size distribution of carboxyl- and amino-functionalized polystyrene particles prepared by miniemulsion polymerization. Langmuir 2007;23:5367–76.
[45] Nałęcz-Jawecki G, Grabińska-Sota E, Narkiewicz P. The toxicity of cationic surfactants in four bioassays. Ecotoxicol Environ Saf 2003;54:87–91.
[46] Vijayendran BR. Effect of carboxylic monomers on acid distribution in carboxylated polystyrene latices. J Appl Polym Sci 1979;23:893–901.
[47] Hen J. Determination of surface carboxyl groups in styrene/itaconic acid copolymer latexes. J Colloid Interface Sci 1974;49:425–32.
[48] Hsu DD, Xia WJ, Song J, Keten S. Glass-transition and side-chain dynamics in thin films: explaining dissimilar free surface effects for polystyrene vs poly(methyl methacrylate). ACS Macro Lett 2016;5:481–6.
[49] Schork FJ, Luo YW, Smulders W, Russum JP, Butté A, Fontenot K. Miniemulsion polymerization. Adv Polym Sci 2005;175. 129-255.
[50] Zhang XQ, Zhang XY, Tao L, Chi ZG, Xu JR, Wei Y. Aggregation induced emission-based fluorescent nanoparticles: fabrication methodologies and biomedical applications. J Mater Chem B 2014;2:4398–414.
[51] Wang XF, Chen YW, Zhou WH, Huang ZF, Guo ZP, Hu YH. A versatile approach for the fabrication of Au hollow nanoparticles based on poly(styrene-*co*-2-aminoethyl methacrylate) template. J Mater Sci 2009;44:4710–4.